Modelling of Four-Junction Solar Cells with a Silicon-Germanium-Tin Subcell

Laurier S. Baribeau, Christopher E. Valdivia, Matthew M. Wilkins, Karin Hinzer
SUNLAB, Centre for Research in Photonics, University of Ottawa, Ottawa, ON, Canada

Abstract — **This paper discusses the simulation of a monolithic four-junction solar cell that incorporates a new semiconducting alloy, SiGeSn. The methodology of developing a simulation involving this material within the context of Synopsys Sentaurus TCAD software is presented. Additionally, design considerations for the solar cell are discussed. Simulation results including the current-voltage characteristics of the solar cell are shown, demonstrating the potential for SiGeSn to be an important contributor to the next generation of solar cells.**

Keywords — **SiGeSn; Group IV; photovoltaics; III-V; TCAD simulation; 4-junction; bandgap engineering; high efficiency**

I. Introduction

Designs of monolithic multi-junction solar cells are often constrained by the limited selection of available semiconductors. $Si_xGe_{1-x-y}Sn_y$ is a material system that has been difficult to grow epitaxially until recently due to the low solubility of tin in germanium. Investigations have shown that this material system includes lattice-matched compositions having ~1.0-eV bandgaps suitable for the third subcell within a four-junction solar cell, extending the standard InGaP/InGaAs/Ge triple-junction design. The proposed heterostructure may also integrate well into low-defect growth on silicon wafers, which is an approach that will realize reduced manufacturing costs through the elimination of expensive Ge wafers. Accurate simulation of such a material within this solar cell architecture will provide insight into the parameters of the design and allow for optimization, a key part of the development process.

II. Model and Structure Description

Simulations are performed using Synopsys Sentaurus. The structure of the solar cell model is shown in Table 1.

A. SiGeSn Material Parameters

Characterization data for this new material system is slowly becoming available. Pearce et. al. provide detailed characterization including ellipsometry-based determination of the complex dielectric function and absorption coefficient. This data was used to calculate the complex refractive index of SiGeSn with a composition of approximately 14% silicon and 3.8% tin. The plot of the absorption coefficient allows for more precise determination of the imaginary part of the complex refractive index for the important spectral region near the band edges. Data from the two fitting methods were used together to compile the complex refractive index values, n and κ, used by Sentaurus in the simulation.

The indirect bandgap of SiGeSn is calculated by Sentaurus using the Varshni equation. For this simulation, these parameters

TABLE I. Solar Cell Structure

Design Component	Region	Material	Thickness [μm]	Dopant Type	Dopant Concentration [cm^{-3}]
Anti-Reflection Coating	Layer 1	MgF	0.100	-	-
	Layer 2	TiO	0.060	-	-
Subcell 1	FSF	$Al_{0.5}In_{0.5}P$	0.025	n	$6x10^{18}$
	Emitter	$Ga_{0.5}In_{0.5}P$	0.100	n	$5x10^{18}$
	Base	$Ga_{0.5}In_{0.5}P$	0.650	p	$8x10^{16}$
	BSF	$Al_{0.125}Ga_{0.375}In_{0.5}P$	0.050	p	$3x10^{19}$
Tunnel Junction 1		$Al_{0.3}Ga_{0.7}As$	0.030	p	$2x10^{20}$
		$Ga_{0.5}In_{0.5}P$	0.030	n	$6x10^{19}$
Subcell 2	FSF	$Al_{0.8}Ga_{0.2}As$	0.030	n	$1x10^{19}$
	Emitter	GaAs	0.100	n	$3x10^{18}$
	Base	GaAs	1.400	p	$1x10^{17}$
	BSF	$Al_{0.2}Ga_{0.8}As$	0.080	p	$1x10^{19}$
Tunnel Junction 2		$Al_{0.3}Ga_{0.7}As$	0.030	p	$1.2x10^{20}$
		GaAs	0.030	n	$6x10^{19}$
Subcell 3	FSF	GaAs	0.050	n	$7x10^{17}$
	Emitter	$Si_{0.14}Ge_{0.82}Sn_{0.04}$	0.100	n	$1x10^{19}$
	Base	$Si_{0.14}Ge_{0.82}Sn_{0.04}$	0.850	p	$1x10^{18}$
Tunnel Junction 3		$Al_{0.3}Ga_{0.7}As$	0.030	p	$1.2x10^{20}$
		GaAs	0.030	n	$6x10^{19}$
Subcell 4	FSF	GaAs	0.050	n	$7x10^{17}$
	Emitter	Ge	0.100	n	$1x10^{19}$
	Substrate	Ge	170	p	$1x10^{18}$
Acronyms	FSF: Front Surface Field. BSF: Back Surface Field				

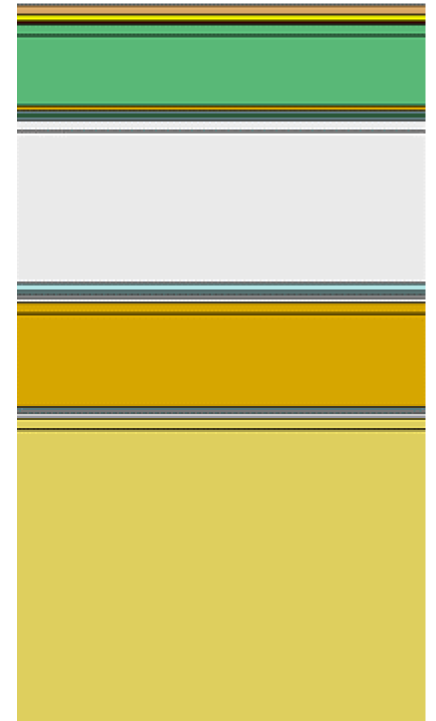

Fig. 1: Visualization of epitaxial growth. Substrate region is truncated and not to scale.

were chosen such that a bandgap of 0.77 eV is achieved at 300 K in accordance with the value inferred from photoluminescence of $Si_{0.14}Ge_{0.82}Sn_{0.04}$ in Pearce et. al.

This composition of SiGeSn was chosen based on preliminary calculations of the desired bandgap, the availability of growth material, and the estimated absorption of the input spectrum (necessary to current-balance with the other subcells). The relative amounts of silicon, tin, and germanium are such that the alloy will lattice-match to germanium with minimal strain, according to Vegard's law.

Additional material parameters were assumed to be similar to those of Germanium. As such, the simulation will continue to be refined as more characterization becomes available.

B. *Sentaurus Device Simulation Physics*

The following physics options, among others, are enabled within the Sentaurus Device simulation: thermionic emission, Shockley-Read-Hall, Auger, and radiative recombination, doping dependent mobility, surface recombination at the TiOx/AlInP interface, and bandgap narrowing. The tunnel junctions are simulated using the nonlocal tunneling model.

The current-voltage characteristics of the subcells are determined by monitoring virtual contacts placed at the cathode, anode, and within each of the tunnel diodes, while a quasistationary voltage ramp is applied to the device.

III. Results & Discussion

The current-voltage characteristics of the four subcells resulting from the simulation are depicted in figure 2. The illumination was simulated with the AM1.5D spectrum with an intensity of 1000 W/cm2 (i.e. 1 sun).

The open circuit voltage of the SiGeSn subcell (0.46 V) is greater than what would be achieved by a germanium subcell in the same position (0.36 V.) Upon further design optimization, this may allow for marked improvement to overall device efficiency. The overall efficiency calculated in this simulation is 36.2%.

The top cells' thicknesses have been slightly reduced such that excess light passes through to the bottom cells and every cell produces similar current in accordance with the current matching requirement of monolithic multi-junction solar cells. Further optimization of the material bandgaps is preferable to meeting the current matching requirement by adjusting the subcell thicknesses, and will be possible after further development of the carrier diffusion length model.

IV. Acknowledgement

This work has been financially supported by grant NSERC STPGP 413276.

V. References

[1] P. Pearce, T. Wilson, A. Johnson, and N. Ekins-Daukes, "Characterization of SiGeSn for Use as a 1 eV Sub-Cell in Multi-Junction Solar Cells." *2018 IEEE 7th World Conference on Photovoltaic Energy Conversion (WCPEC)(A Joint Conference of 45th IEEE PVSC, 28th PVSEC & 34th EU PVSEC)*. IEEE, 2018.

[2] A. Attiaoui and O. Moutanabbir, "Indirect-to-direct band gap transition in relaxed and strained $Ge_{1-x-y}Si_xSn_y$ ternary alloys." *Journal of Applied Physics*116.6 (2014: 063712.

[3] M. Wilkins, C. E. Valdivia, A. M. Gabr, D. Masson, S. Fafard, and K. Hinzer, "Luminescent coupling in planar opto-electronic devices." *Journal of Applied Physics* 118.14 (2015): 143102.

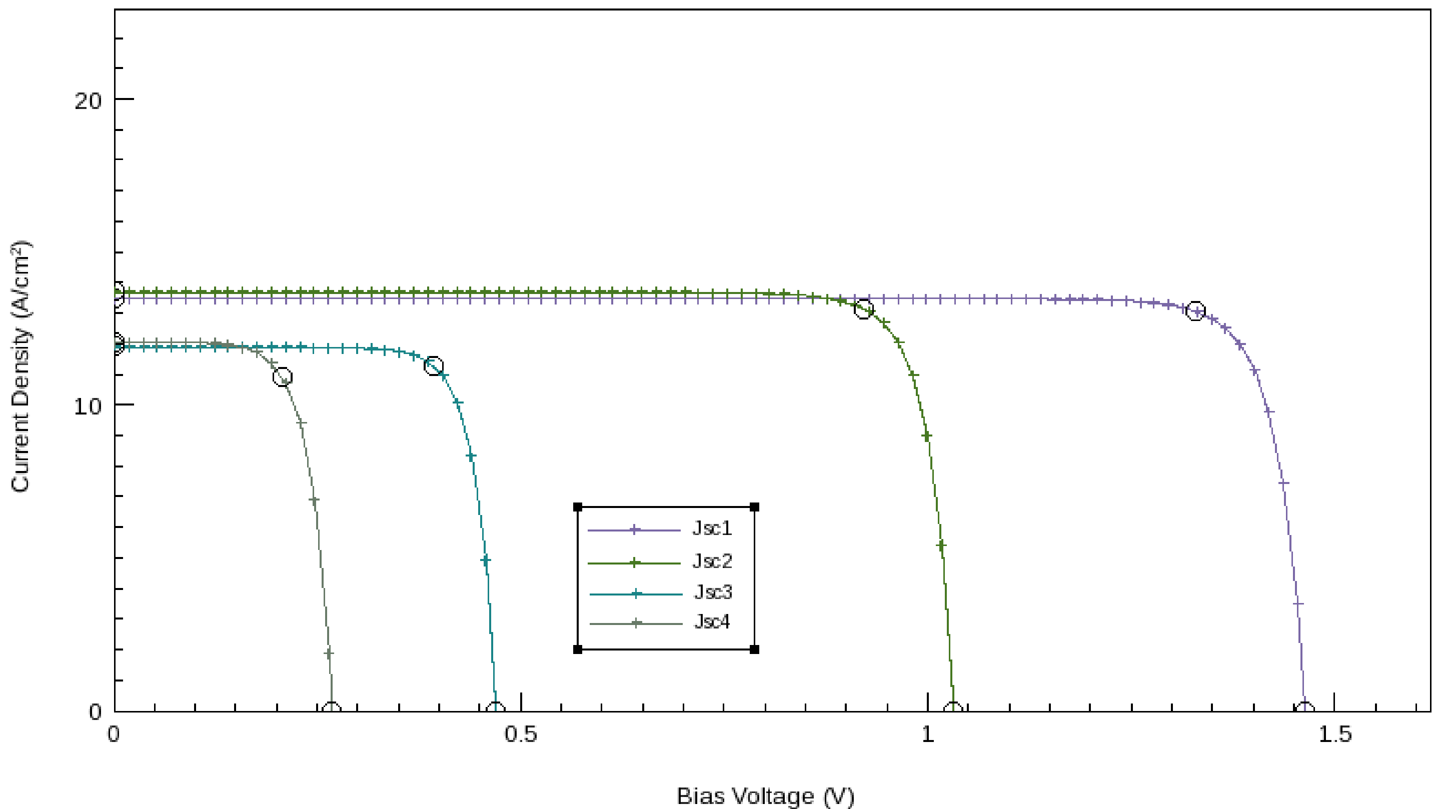

Fig. 2: Current-voltage characteristics of the four subcells. Maximum power points are shown.